

NAL PROPOSAL No. 0056

Correspondent: R. L. Cool  
Brookhaven National Lab  
Upton, L.I., N.Y. 11973

FTS/Commercial 516-924-2237

MEASUREMENT OF TOTAL CROSS SECTIONS ON HYDROGEN AND DEUTERIUM

R. L. Cool, S. Segler  
Rockefeller University

A. S. Carroll, T. F. Kycia, K. K. Li, D. N. Michael, P. M. Mockett  
R. Rubinstein  
Brookhaven National Laboratory

June 12, 1970

NAL PROPOSAL

Measurement of Total Cross Sections on Hydrogen and Deuterium

ABSTRACT

Total cross sections of  $\pi^+$ ,  $K^+$ ,  $p$  and  $\bar{p}$  on hydrogen and deuterium are to be measured at about eight energies between 20 GeV and the maximum available energy. An accuracy of about one part in one thousand will yield the energy dependence of cross sections, comparisons of cross sections within SU(3) supermultiplets, and stringent tests of high energy limiting theorems.

R.L. Cool and S. Segler

Rockefeller University

A.S. Carroll, T.F. Kycia, K.K. Li, D.N. Michael, P.M. Mockett,

and R. Rubinstein

Brookhaven National Laboratory

June 12, 1970

Correspondent: R.L. Cool

We propose, as a continuation of our studies at Cosmotron and AGS energies, to measure the total cross sections of  $\pi^+$  and  $\pi^-$ ,  $K^+$  and  $K^-$ , and  $p$  and  $\bar{p}$  on hydrogen and deuterium from about 20 GeV to the maximum energy available at NAL. Accurate measurements of this basic parameter of strong interactions are an essential ingredient to the understanding of phenomena at very high energies; their behavior as a function of energy is a direct test of general limiting theorems.

It does not seem necessary, in view of the wide literature on the subject, to present a detailed argument on the possible interpretations to be given to the energy dependence of the total cross sections which might be observed. We mention only a few of the general physical principles which can be tested, namely:

- (1) The Pomeranchuk theorem which predicts that  $\sigma(\pi^+p) = \sigma(\pi^-p)$ ;  $\sigma(K^+p) = \sigma(K^-p)$ ; and  $\sigma(pp) = \sigma(\bar{p}p)$  at sufficiently high energy.
- (2) The Pomeranchuk theorem which predicts that  $\sigma(pp) = \sigma(pn)$ ;  $\sigma(\pi^+p) = \sigma(\pi^+n)$ , etc., at sufficiently high energy.
- (3) Charge independence of strong forces which predicts  $\sigma(\pi^+d) = \sigma(\pi^-d)$  at all energies.

As in our previous experiments, the deuteron Glauber-Wilkin shielding correction is determined from the pion-proton and pion-deuteron cross sections. The cross sections as a function of energy for each pure isospin state can then be deduced for K mesons, protons and antiprotons.

The imaginary part of the forward scattering amplitude as a function of energy is computed directly. The real part of the forward scattering amplitude can be computed via the dispersion relations and tested with considerable accuracy against direct measurements of this quantity. The real

and imaginary amplitudes give directly the  $\pi^- p \rightarrow \pi^0 n$  and  $\pi^+ n \rightarrow \pi^0 p$  charge exchange cross sections and the regeneration of  $K_S^0$  from  $K_L^0$  on hydrogen and deuterium which can be tested by other experiments.

It has been noted that the new measurements available from Serpukhov which extend earlier work at the AGS and at CERN to the 50-70 GeV region already raise some doubt as to whether the limiting theorems of constancy of total cross section and equality of cross sections for members of the same SU(3) supermultiplets can be applied. Both the increased energy range at NAL and the possibility of increasing considerably the accuracy of the data can provide a much more severe test of current ideas.

#### Experimental Method

We wish to stress the need for, and the possibility to achieve, great accuracy in the measurements. In order to be able to make the comparisons of cross sections indicated in the introduction, it is necessary that:

(1) The energy dependence of a given cross section over the full range should have a relative accuracy of 10-30  $\mu$ b. The lower value applies for the more abundant particles ( $\pi^+$ , p) and the upper for the less abundant ( $K^+$ ,  $\bar{p}$ ). Such accuracy requires excellent angular resolution for the extrapolation of measurements of partial cross sections at finite solid angles to zero solid angle, and we believe this can be aided by the use of proportional wire chambers (PWC) in addition to the standard scintillation counters.

(2) The comparison of the same isospin multiplet on a given target, say  $\sigma(\pi^+ p)$ , to an accuracy of 20-40  $\mu$ b requires extreme stability not only

of electronic and magnetic components, but also of target density. Corrections for multiple and single Coulomb scattering as well as beam contamination at this level must be known with sufficient accuracy from the data, or subsidiary measurements.

(3) For the absolute cross sections on hydrogen and deuterium, we believe it reasonable to aim at an accuracy of about one part per thousand. In addition to the requirements of (1) and (2) above, this accuracy requires that the absolute density of the hydrogen and deuterium targets (as well as their physical length) be known to better than one per mil. We also expect to recheck and, if necessary, remeasure the vapor pressure vs. density curves for deuterium which may have been the cause of previous discrepancies between various laboratories in absolute cross section measurements.

We detail now the physical layout and the methods by which we consider that we can achieve the accuracies listed above.

A schematic layout of the apparatus is shown in Fig. 1. The incoming particle is defined in direction by PWC 1, PWC 2, and PWC 3, each of which consists of a module comprising four planes of proportional wire chambers. The Cerenkov counter (or counters) C1, placed before the quadrupoles Q1 and Q2, measures the velocity of the incoming particle and, together with the beam momentum, defines its identity. The targets (T) consist of three identical modules (one for hydrogen, one for deuterium, and one a dummy) capable of being placed easily in the beam in rotation. The unscattered particles and those which scatter less than an angle  $\theta_{\max}$  are detected in modules PWC 4 and PWC 5. The large absorber block (A) following PWC 5 is used to define the muon contamination as described below. Scintillation counters SC1, SC2, SC3 define the beam and, in coincidence with C1, provide

the trigger for the PWC modules. The counter set SC4 consists of several counters of different diameter to measure the transmitted beam in the standard way. Counter SC5, together with the beam defining counters, measures the muon contamination of the beam. The counter set SC4, PWC 5, A, and SC5 are mounted on a cart which is moved along the beam line on rails. For each momentum the cart is moved so that the transmission counters SC4 subtend the same range of  $-t$ .

For scattering angles which correspond to momentum transfers larger than approximately  $0.1 \text{ (GeV/c)}^2$ , the partial cross sections are measured in the standard way by the transmission counters SC4. Thus full advantage can be taken of the high rate of data acquisition for which counters are best suited. For momentum transfers smaller than approximately  $0.1 \text{ (GeV/c)}^2$ , the PWCs are interrogated by a coincidence of the beam telescope and counters of SC4 corresponding to this range of momentum transfer. The great spatial resolution of the chambers will make possible accurate extrapolation for small momentum transfers. The PWCs are limited to a few hundred events per pulse by data acquisition and are thus used only to provide the slope at small angles.

We shall provide a PDP-15 computer to monitor all relevant parameters of the experiment including beam magnets, target vapor pressure, high voltages, beam spill, etc. The buffer memory will be read onto tape between pulses when all parameters for that pulse fall within tolerance. Thus the need, for example, for long runs under rigid beam spill requirements can be eliminated, bad pulses simply being erased from the buffer without being accumulated on tape. It is our experience that this method will maintain rigid control of the parameters pulse by pulse, making maximum use of beam time, and keep the data in statistical control. In

normal practice, long runs often must be eliminated post facto which results in inefficient beam utilization.

For the coordinate data, scattering angles will be computed on and off line as required to accumulate the data for the particles scattered at small angles. From these data, accurate extrapolation to zero solid angle should be possible.

#### Measurements

We propose initially to measure  $\sigma_T$  for the six particle types with the two targets of H and D at each of eight energies, a total of  $6 \times 2 \times 8 = 96$  measurements. Depending on the energy at which the accelerator operates, the measurements would be spaced at intervals between 25 and 50 GeV. Absorption cross sections for complex nuclei can be measured during the course of the experiment with negligible increase in running time.

For purposes of estimating rates, we take a conservative value of  $1.5 \times 10^5$  particles traversing the apparatus per pulse. Such a value is tolerable for a spill length of 300-500 msec and would have to be adjusted to prevailing conditions. Special electronic gating techniques which we have used before will prevent pile-up in scalars and insure PWC recovery.

For a target length of 5 meters, the fractional statistical error is given approximately by

$$\frac{\Delta\sigma}{\sigma} \approx \frac{3}{\sqrt{N}}$$

where N is the total number of incident particles. Thus, to achieve a statistical precision of one part in 2000 requires approximately  $4 \times 10^7$  incident beam counts. The total beam per hour would be

$$1.5 \times 10^5 \times 15 \times 60 \approx 10^8,$$

so that a typical data run would be about fifteen minutes for  $\pi^+$  and p, and about ten to twenty hours for  $K^+$  and  $\bar{p}$ .

For  $\pi^+$  and p with short data runs, we know from experience that the time required will be completely dominated by setting bending and focusing magnet currents and Cerenkov counter pressure, by efficiency checks, by multiple runs to crosscheck stability, and by dummy target runs. We also estimate that for the extrapolation about  $10^6$  PWC events are needed. Based on 500 events per pulse,  $\sim 2$  hr is required for this purpose. Taking all into account, each data point will need  $\approx 6$  hr.

For the  $K^+$  and  $\bar{p}$ , where the effective beam is reduced between a factor of 30 and 100, the data accumulation will require a more significant fraction of the time. An average time of 15 hr per point is estimated.

The total time required is then  $\approx 1,000$  hours.

#### Special Equipment

I. Particle Identification. The incident beam particle will be defined by means of Cerenkov counters, which we are prepared to design and construct. A differential Cerenkov counter can be built of sufficient resolving power for our needs, but its detailed design is greatly affected by the divergence of the beam in which it is placed; for instance, with a beam divergence of  $\pm 0.2$  mr a differential counter of length  $\sim 20$  meters would be sufficient. Since the counter and beam design are so interdependent, we would be willing to assist in the latter if requested. In a worst case where a beam of sufficient parallelism is not available, the experiment could still be carried out adequately using threshold Cerenkov counters.

II. Beam. The beam which has been considered for this proposal was the 200-GeV/c beam described by D. Reeder and J. MacLachlan in SS-41. The solid angle of acceptance,  $\Delta\Omega$ , was taken to be  $10^{-6}$   $\mu$  sr. For  $10^{12}$  protons interacting on the production target the available range in momentum spread  $\pm 0.017\% \leq \frac{\Delta p}{p} \leq 1\%$  would be adequate to provide  $1.5 \times 10^5$  particles per pulse over the full momentum range for a positive beam and up to 160 GeV/c for the negative beam.

III. Targets. The targets would be similar to those developed in our last few total cross-section experiments. The vessels containing the liquid hydrogen and liquid deuterium are contained inside an outer cylinder filled with liquid hydrogen. The vapor pressure of the outer liquid would be regulated to within  $\pm 0.07$  psi. This pressure fluctuation would correspond to a density fluctuation of  $\pm 0.05\%$  for the inner hydrogen and deuterium. The absolute densities and lengths of the targets will be established to better than  $\pm 0.1\%$ . A third, dummy target would be used for background subtraction. The optimum target length is calculated to be about five meters; a target diameter of three inches may be sufficient.

Since we anticipate the long-term need by NAL for Cerenkov counters and targets of the general type required for this proposal and since we have accumulated substantial experience over several years in the design of this type of equipment, we propose to design and build them and to turn them over to NAL for general use following the experiment, should this be desirable. Alternatively, we are prepared to utilize NAL-designed equipment, if available. Methods of meeting special NAL requirements for safety, etc., and financing arrangements need to be worked out with NAL, BNL and the AEC if we are to undertake design and construction responsibility.

### Personnel

In addition to the scientists listed by name on the proposal, we expect to be joined by approximately 2 Ph.D.-level staff members and 1 graduate student from Rockefeller University. We would be prepared to add a few additional collaborators from NAL or other universities.

### Related Experiments

Except for overlap with existing data at lower energies from BNL, CERN and Serpukhov for checking purposes, most of the data will be unique to NAL. The CERN ISR can, in principle, measure p-p total cross sections over the same range. Two experiments have been approved there for this purpose.

### Time Scale

Approximately one year will be required to build and test the necessary equipment. Design could begin when approval is indicated.

### Summary

We believe that measurements of the total cross sections will play a basic role in the understanding of strong interactions in the new energy range and that the need for accuracy must be stressed if clear conclusions are to be drawn. Moreover, we regard it as essential that the full set of the measurements be made in a consistent manner to permit cross comparison.

The beam requirements on intensity and dispersion in momentum are not severe. Our electronics is designed with special precautions to allow us to take satisfactory data under varying duty cycle conditions. For these reasons we believe the proposed work could be undertaken at a relatively early stage following accelerator turn-on.

BROOKHAVEN NATIONAL LABORATORY

BY..... DATE.....

SUBJECT.....

SHEET No..... OF.....

CHKD. BY..... DATE.....

DEPT. OR PROJECT.....

JOB No.....

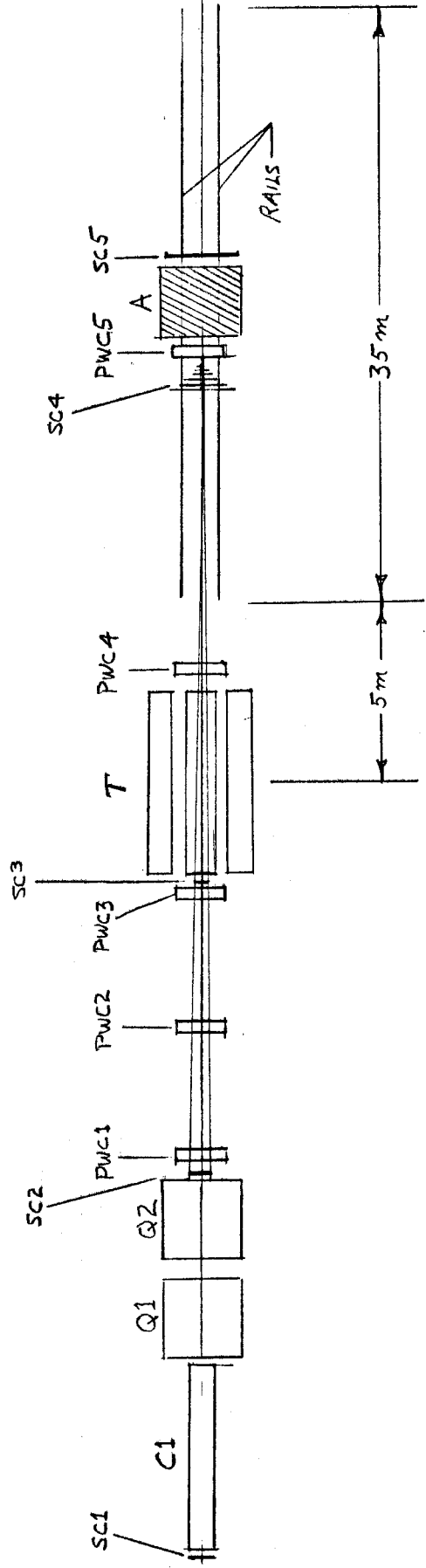


FIGURE 1

APPENDIX A

Real Parts of Meson-Nucleon Forward Scattering Amplitudes\*

D. HORN\*\* and A. YAHIL

California Institute of Technology, Pasadena, California 91109

(Received January , 1970)

ABSTRACT

A dispersion relation calculation of the real parts of forward  $\pi^+p$  and  $K^+p$  scattering amplitudes is carried out under the assumption of constant total cross sections in the Serpukhov energy range. Comparison with existing experimental results as well as predictions for future high energy experiments are presented and discussed. Electromagnetic effects are found to be too small to account for the expected difference between the  $\pi^-p$  and  $\pi^+p$  total cross sections at higher energies.

\*Work supported in part by the U. S. Atomic Energy Commission. Prepared under Contract AT(11-1)-68 for the San Francisco Operations Office, U. S. Atomic Energy Commission.

\*\*On leave of absence from Tel Aviv University, Tel Aviv, Israel.

## I. INTRODUCTION

The recent Serpukhov experiments<sup>1)</sup> show that all measured meson-nucleon total cross sections stay constant at energies above 30 BeV. This contradicts previous expectations from theories describing the behavior of the cross sections at energies below 30 BeV. In the present paper, we investigate the effect of the new results on the real parts of meson-nucleon scattering amplitudes via dispersion relations. We analyze the  $\pi^{\pm}p$  system following the approach developed in Ref. 2. We discuss the phase of the forward  $\pi^{\pm}p$  scattering amplitudes as well as the forward differential cross section of  $\pi N$  charge exchange (CEX). We find an estimate for the upper limit of electromagnetic effects in these amplitudes, and conclude that it is too small to account for the expected difference between  $\sigma_T(\pi^-p)$  and  $\sigma_T(\pi^+p)$  at the higher energies. We discuss the fits to presently available data and make predictions for future high-energy experiments. We treat  $K^{\pm}p$  scattering in a similar way. Although the experimental data on the real parts of the amplitudes are not very accurate, they favor the existence of an additional term. This would be implied if the difference between  $\sigma_T(K^-p)$  and  $\sigma_T(K^+p)$  persists at higher energies.

It should be noted that in order to evaluate the real part, it is only necessary to speculate on the behavior of the total cross sections up to energies which are, say, an order of magnitude greater. A different extrapolation beyond there does not necessarily affect the dispersion calculation.

In Section II we present the general formalism and discuss a mathematical example that is close to the real situation in  $K^{\pm}p$ . In Section III we treat the  $\pi p$  problem in detail. Section IV deals with the  $Kp$  system.

## II. GENERAL FORMALISM

We use dispersion relations to analyze a  $t = 0$  scattering amplitude, whose discontinuity is determined by total cross sections of two channels related by crossing (e.g.,  $\pi^+p$  and  $\pi^-p$  or  $K^+p$  and  $K^-p$ ). We refer the reader to Ref. 3 for the conventional formulation of dispersion relations and previous calculations. One separates the symmetric amplitude  $A^{(+)} = \frac{1}{2} [A(\pi^-p) + A(\pi^+p)]$  from the antisymmetric one  $A^{(-)} = \frac{1}{2} [A(\pi^-p) - A(\pi^+p)]$ , and writes the dispersion relations

$$A^{(+)}(\nu) = A^{(+)}(\mu) + \frac{f^2 k^2}{M \left[ 1 - \left( \frac{\mu}{2M} \right)^2 \right] \left[ \nu^2 - \left( \frac{\mu}{2M} \right)^2 \right]} + \frac{k^2}{2\pi^2} \int_{\mu}^{\infty} \frac{\nu' \sigma^{(+)}(\nu')}{\nu'^2 - \nu^2 - i\epsilon} d\nu' \quad , \quad (1)$$

$$A^{(-)}(\nu) = \frac{2f^2 \nu}{\nu^2 - \left( \frac{\mu}{2M} \right)^2} + \frac{\nu}{2\pi^2} \int_{\mu}^{\infty} \frac{k' \sigma^{(-)}(\nu')}{\nu'^2 - \nu^2 - i\epsilon} d\nu' \quad . \quad (2)$$

$M$  is the nucleon mass and  $\mu$  the meson mass.  $\sigma^{(\pm)} = \frac{1}{2} [\sigma_{\mathbb{T}}(\pi^-p) \pm \sigma_{\mathbb{T}}(\pi^+p)]$ .

$\nu$  and  $k$  are the meson's laboratory energy and momentum respectively.

$f^2$  specifies the strength of the Born term, and is equal to 0.082.

$A^{(+)}(\nu = \mu)$  is the only subtraction constant. It is known to be zero within experimental errors, in agreement with Adler's PCAC self-consistency condition.<sup>4)</sup> In writing (2), one obviously makes the assumption that  $\sigma^{(-)}$  goes asymptotically to zero. This is the point which we now want to change. Following the approach of Ref. 2, we assume that both  $\sigma_{\mathbb{T}}(\pi^-p)$  and  $\sigma_{\mathbb{T}}(\pi^+p)$  remain constant from about 30 BeV on. This then implies that they have different values, and  $\sigma^{(-)}$  is a non-zero constant. We want to

see what the predictions of these assumptions for the real part are.

Having to introduce a subtraction into (2), we therefore replace it by

$$\begin{aligned}
 A^{(-)}(\nu) = & \frac{2 f^2 \nu}{\nu^2 - \left(\frac{\mu}{2M}\right)^2} + \frac{\nu}{2\pi^2} \int_{\mu}^{\kappa} dv' \frac{k' \sigma^{(-)}(\nu')}{\nu'^2 - \nu^2 - i\epsilon} \\
 & + \frac{\nu k^2}{2\pi^2} \int_{\kappa}^{\infty} dv' \frac{\sigma^{(-)}(\nu')}{k' (\nu'^2 - \nu^2 - i\epsilon)} + c \frac{\nu}{M^2} . \quad (3)
 \end{aligned}$$

Note that, instead of performing a subtraction on the entire integral, we divide it into two parts. One is written in an unsubtracted form, and the other in a subtracted one. This is done for practical purposes. It avoids stressing the low-energy input and thus increasing the errors in the calculation. The number  $c$  depends on the choice of  $\kappa$ . Equation (3) also demonstrates the fact that the real part at low energy is not necessarily affected by the new assumptions on the high-energy behavior. We are actually able to reproduce at low energies (say, below 4 BeV) the same results previously obtained by the use of (2) with any reasonably decreasing fit to  $\sigma^{(-)}$ .

To illustrate the changes brought about by the assumptions on the behavior of the total cross section, let us discuss a mathematical example that is very similar to the actual situation in  $K^+p$ . Let us denote the two reactions in question by A and B (analogous to  $K^+p$  and  $K^+n$  respectively). Assume first that (case I):

$$\text{Im } A_I = a \nu \quad , \quad \text{Im } B_I = a \nu + b \sqrt{\nu} \quad , \quad 0 < \nu < \infty \quad . \quad (4)$$

It is then easy to find that

$$\text{Re } A_I = - b \sqrt{\nu} \quad , \quad \text{Re } B_I = 0 \quad . \quad (5)$$

This is the expected result for  $K_{\text{I}}^{\pm}$  if one uses a Regge representation with a regular Pomeron and two pairs of exchange degenerate trajectories with intercepts at  $1/2$ . If we now make the analogous assumption to that of Ref. 2, we have (case II):

$$\text{Im } A_{\text{II}} = a v \quad , \quad \text{Im } B_{\text{II}} = \begin{cases} a v + b \sqrt{v} & 0 < v < \Lambda \\ \left(a + \frac{b}{\sqrt{\Lambda}}\right) v & \Lambda < v < \infty \end{cases} \quad (6)$$

It is then readily established that

$$\begin{aligned} \text{Re } A_{\text{II}} &= -\frac{2b\sqrt{v}}{\pi} \arctan \sqrt{\frac{\Lambda}{v}} + \frac{b v}{\pi \sqrt{\Lambda}} \log |v + \Lambda| - \frac{c}{M^2} v \quad , \\ \text{Re } B_{\text{II}} &= \frac{b\sqrt{v}}{\pi} \log \left| \frac{\sqrt{v} - \sqrt{\Lambda}}{\sqrt{v} + \sqrt{\Lambda}} \right| - \frac{b v}{\pi \sqrt{\Lambda}} \log |v - \Lambda| + \frac{c}{M^2} v \quad . \end{aligned} \quad (7)$$

It is now interesting to note that although Eqs. (5) and (7) are very different from one another, it is still possible to find a value of  $c$  that will show a similar behavior for low  $v$ . Thus it is possible that even though  $\text{Im } B_{\text{I}} \neq \text{Im } B_{\text{II}}$  for  $v > \Lambda$ , one still finds that the real parts of the various amplitudes can roughly agree for  $v < \Lambda$ .

To illustrate this point numerically, we choose  $a = b = 3.6$ ,  $\Lambda = 22$ . (These values are <sup>indicated</sup> by experiment if  $v$  is measured in BeV and the amplitudes in  $\text{BeV}^{-1}$ .) We find such an agreement between I and II for  $c = 1.1$ . We present in Fig. 1 the results for  $\alpha(A) = \text{Re } A / \text{Im } A$  and  $\alpha(B) = \text{Re } B / \text{Im } B$ , since this is the customary way in which the data are given in  $\pi N$  experiments.

Note that after the value  $v \approx 100$  the logarithmic part in  $\text{Re } A_{\text{II}}$  and  $\text{Re } B_{\text{II}}$  is taking over. Nevertheless it does not reach a sizable amount even at high  $v$  values. To quote a number -- at  $v = 10^6$  we find

$\alpha(B_{II}) = -0.49$  and  $\alpha(A_{II}) = 0.59$ . We will find a similar behavior in the next section when discussing the  $\pi N$  problem.

### III. REAL PARTS OF $\pi^{\pm}p$ AMPLITUDES

In Ref. 2, the  $\pi^{\pm}p$  total cross sections were fitted to a form

$$\sigma_{\pm} = a_{\pm} + b_{\pm}/\sqrt{\nu} \quad . \quad (8)$$

An ionization point was then assumed to appear at  $\nu = 30$  BeV, resulting in the flattening off of the cross sections at that point. This meant that  $2\sigma^{(-)} = \sigma(\pi^{-}p) - \sigma(\pi^{+}p) > 1$  mb even at high energies. In Ref. 2,  $\sigma^{(-)}$  was assumed to remain a constant for  $\nu \geq 30$  BeV.

Any breaking of the Pomeranchuk theorem results in a logarithmic rise of the real part of the amplitude, notably of  $A^{(-)}(\nu)$ .<sup>2,5)</sup> Hence  $\alpha_{\pm}(\nu) = \text{Re } A_{\pm}(\nu)/\text{Im } A_{\pm}(\nu)$  does not tend to 0 as  $\nu \rightarrow \infty$ . Once the logarithmic behavior begins to dominate,  $\alpha$  rises in absolute value, with  $\alpha_{+}$  and  $\alpha_{-}$  taking opposite signs. The strength of the logarithmic term is proportional to the value of  $\sigma^{(-)}$ .

The dispersion integrals were evaluated on a computer. In order to do the principal part integration, it is necessary to have a smooth fit to the data points, since the integral is sensitive to discontinuities near  $\nu' = \nu$ . For  $\nu \leq 4$  BeV we used the fit of Ref. 3. The data between 4 and 30 BeV<sup>6,7)</sup> can be fitted in a variety of ways. We first fitted each cross section separately to a form

$$\sigma_{\pm} = a_{\pm} + b_{\pm} \nu^{n-1} \quad . \quad (9)$$

In such fits,  $a_{-} - a_{+}$  was invariably greater than 1 mb, and the choice of  $n$  was a matter of taste. We then tried a fit satisfying the Pomeranchuk theorem

$$\sigma_{\pm} = a + b v^{n-1} \pm c v^{m-1} \quad . \quad (10)$$

This was done in order to be able to compare the premise of a cutoff with the assumption that the Serpukhov data might be wrong, and that the Pomeranchuk theorem might be right after all.

The data of Citron et al.<sup>6)</sup> do not seem to fit smoothly to those of Foley et al.<sup>7)</sup>. We had to settle for a slightly low value of  $n$ . We chose

$$n = 0.25 \quad , \quad m = 0.6 \quad .$$

Applying to fit (10) a cutoff at 30 BeV, we got for  $v$  above cutoff

$$2\sigma^{(-)} = \sigma(\pi^{-}p) - \sigma(\pi^{+}p) = 1.3 \text{ mb} \quad .$$

This number is consistent with the result of Ref. 1. In doing the same with fit (9), we got  $2\sigma^{(-)}$  above cutoff to depend on the fit.  $\sigma(\pi^{-}p)$  is, of course, determined by the Serpukhov data, but there is a slight freedom of play in  $\sigma(\pi^{+}p)$ . We assumed the cutoff point to be the same as in  $\pi^{-}p$  (30 BeV) and since this is 8 BeV higher than the last data point, the extrapolation depends on the fit. If we constrained fit (9) to satisfy  $2\sigma^{(-)} = 1.3 \text{ mb}$ , the dispersion relations gave the same results for the real parts as fit (10). We adopted the latter for the purpose of testing the sensitivity of the calculation to the possible breaking of the Pomeranchuk theorem. We called case I that which assumes (10) to be good for all  $v$ . In case II we applied the cutoff, so that for  $v \geq 30 \text{ BeV}$  both cross sections were constant. The two cases are illustrated in Fig. 2. Note that if further structure appears in  $\sigma_T$  at much higher energies, it may have negligible effects on our calculation.

The calculated ratios  $\alpha_{\pm}(v) = \text{Re } A_{\pm}(v) / \text{Im } A_{\pm}(v)$  for the  $\pi^{\pm}p$  amplitudes are plotted in Fig. 3, together with the data.<sup>8)</sup> In case I there

is no free parameter in the dispersion relations (1) and (2). In case II there is the arbitrariness of  $c$  in (3), which can be chosen to best fit the data. (We used  $\kappa = 4$  BeV.)

If one assumes exact charge independence, one can evaluate the forward CEX differential cross section. The predictions are plotted together with the data<sup>9)</sup> in Fig. 4 and Fig. 5. We note that in case I the prediction seems to be too high by about 30% at, say, 20 BeV. If we attribute the discrepancy to I-spin violation of the electromagnetic amplitude, we find it to be 20% of the total  $A^{(-)}$  amplitude. With  $2\sigma^{(-)}(\nu=20) \sim 1.5$  mb, we would thus have  $2\sigma_{EM}^{(-)} \lesssim 0.3$  mb. Since we do not expect the electromagnetic effects to vary strongly with energy, we may conclude that the ansatz of the Pomeranchuk theorem is good only up to  $2\sigma^{(-)}(\infty) \lesssim 0.3$  mb.

In case II one can adjust  $c$  so as to get a very good fit to the CEX data ( $c = 0.35$ ). Alternatively, one can fix  $c$  to fit the  $\alpha_{\pm}$  data. Choosing here  $c = 0.35$ , we find a good fit to  $\alpha_{+}$  but a poor one to  $\alpha_{-}$ . This is an improvement over case I. A change to  $c = 0.25$  results in an equivalent overall fit to  $\alpha_{\pm}$  with a poorer fit to  $\alpha_{+}$  and a better one to  $\alpha_{-}$ . Note that such a change contributes oppositely to  $\alpha_{+}$  and  $\alpha_{-}$ . Checking the CEX prediction with  $c = 0.25$ , we find it too low by about 40%. This corresponds to  $2\sigma_{EM}^{(-)} \lesssim 0.5$  mb.

Note that the small deviations that we found are a feature of our calculated real parts. Point by point, the experimental  $\alpha_{\pm}(\nu)$ , within their errors, are consistent with the CEX data without any I-spin violation. This was already pointed out by Foley *et al.*<sup>8)</sup> Although we can fit the data with no I-spin breaking, we cannot rule out  $2\sigma_{EM}^{(-)} \lesssim 0.5$  mb. However, this is still too small to account for the expected constant difference between  $\sigma_T(\pi^-p)$  and  $\sigma_T(\pi^+p)$ . We have to conclude, then, that this difference is a genuine strong interaction effect.

The main difference between the two dispersion calculations I and II sets in around 100 BeV. At that point, the logarithmic part of  $\text{Re } A^{(-)}$  in case II begins to dominate. Instead of going to zero,  $\alpha_+(v)$  becomes positive and increases, while  $\alpha_-(v)$  turns over and becomes more negative. The CEX forward cross section begins to rise again. On an absolute scale, both effects are small. We should be able to see the CEX forward cross section flattening, but for the real part to dominate the amplitude we will need fantastically high energies. By that time, a new physics may very well set in. It was pointed out in Ref. 2, as well as in Ref. 5, that if  $\text{Re } A/\text{Im } A$  grows logarithmically, then one has to have the forward elastic peak shrink like  $\log^2 s$  to avoid a conflict with unitarity. Strictly speaking, such a conflict would arise only at such large values of  $v$  that the whole problem looks rather academic. Nevertheless, the same conclusion about the shrinkage arises of course from the assumption that  $\sigma_{e1}$  does not rise with energy, which might very well be the case.

Finally, a word about errors and low-energy behavior. The cross sections are accurate to about 1%. This leads to errors of approximately  $\pm 0.003$  in  $\alpha_{\pm}(v)$ . A change in  $\sigma^{(-)}$  above cutoff causes a bigger correction. Varying the high-energy cross sections above 30 BeV does not change the low-energy ( $v \leq 4$  BeV) dispersion calculations. There, our results agree with those of Ref. 3.

#### IV. REAL PARTS OF $K^{\pm}_p$ AMPLITUDES

We calculated the real parts of  $K^{\pm}_p$  forward scattering amplitudes in the same way as for  $\pi^{\pm}_p$ . The data between threshold and  $v = 3.3$  BeV were slightly smoothed. Above that point, the following fit was made:

$$\begin{aligned}\sigma(K^+p) &= a, \\ \sigma(K^-p) &= a + b/\sqrt{\nu}\end{aligned}\tag{11}$$

The dispersion relations were evaluated for cases I and II as in  $\pi p$ , with the cutoff in case II taken at 20 BeV. The errors involved here are much bigger than in  $\pi p$ . The uncertainties in the subthreshold singularities do not allow a good determination of the real parts at low energies. In particular, the  $Y^*(1405)$  is an S-wave, and thus is not quenched kinematically. We estimate its effect to be six times as big as the Born term in  $\pi N$ . This would be approximately 5 - 10% of the real part at  $\nu = 5$  BeV. An additional unknown is the subtraction term of the symmetric amplitude,  $A^{(+)}(\nu=\mu)$ . However, their combined effect remains constant, while the imaginary part grows like  $\nu$ , so that their contribution to  $\alpha(K^+p)$  should fall like  $1/\nu$ . In case II there is the further difficulty of evaluating the subtraction constant  $c$  in the antisymmetric amplitude  $A^{(-)}$ . The CEX reactions are not related by a simple I-spin rotation. Nor has a direct experimental determination of  $\alpha_{\pm}(\nu)$  by Coulomb interference been done. The only existing test is the forward elastic differential cross section. This is a measurement of  $1 + \alpha^2$ . If  $\alpha$  is small, its determination becomes difficult. Fortunately there exists relatively accurate  $K^+p$  data,<sup>10)</sup> which suggests  $|\alpha(K^+p)| \sim 0.55 \pm 0.15$  for  $\nu \sim 7 - 15$  BeV. The error in  $\alpha$  is evaluated by assuming the  $d\sigma/dt$  data to vary within their error bars. If we allow a further variation of one standard deviation, we can set a lower limit on  $\alpha$  of  $\sim 0.25$ . The  $K^-p$  data<sup>11)</sup> is consistent with  $|\alpha(K^-p)| = 0$ , but an upper limit of  $\sim 0.3$  has to be allowed within error bars. An additional standard deviation increases this limit to  $\sim 0.5$ . The

calculated values of  $\alpha(K^+p)$ , together with the experimental limits are plotted in Fig. 6.

Case I seems to disagree with the data. In case II we can explain the discrepancy by means of the subtraction term. To fit  $\alpha(K^+p)$ , we can choose either one of two values, depending on the sign of  $\alpha$ , which cannot be determined by this method. We find for  $\kappa = 3.3$ ,

$$c = \begin{cases} 2 & \alpha(K^+p) < 0, \quad \alpha(K^-p) > 0 \\ -1.6 & \alpha(K^+p) > 0, \quad \alpha(K^-p) < 0 \end{cases} .$$

$c = -1.6$  is ruled out because it gives  $\alpha(K^-p) \sim -0.65$ . Hence we conclude that  $\alpha(K^+p) < 0$  and  $\alpha(K^-p) > 0$ . The data points for  $\alpha(K^+p)$  were plotted under this assumption in Fig. 6. The errors are clearly very large, and allow us to safely ignore the subthreshold singularities.

The general features of  $\pi p$  dispersion relations appear also in  $Kp$ . The logarithmic behavior is magnified because  $2\sigma^{(-)} \sim 4$  mb. However, at present energies the bulk of the real part seems to come from the subtraction term, and not from the logarithmic one. In fact, these appear to have opposite signs. Thus we expect  $|\alpha|$  to actually fall until very high energies, when  $\alpha$  changes signs and  $|\alpha|$  begins to grow again. As in  $\pi p$ , the real part does not dominate until extremely high energies.

The difference between the pion and the kaon amplitudes lies in the energy range below the cutoff point. The usual Regge picture -- which assumes the Pomeranchuk theorem to hold -- is compatible with experiment for the pions, but appears not to be so for the kaons. In the latter case, the existence of an additional real term seems to be implied by the data.

## REFERENCES

1. IHEP-CERN Collaboration, J. V. Allaby et al., Physics Letters 30B, 500 (1969).
2. D. Horn, Caltech report CALT-68-228 (to be published).
3. G. Höhler, G. Ebel, and J. Giesecke, Zeit. f. Physik 180, 430 (1964).
4. S. L. Adler, Phys. Rev. 139, B1638 (1965).
5. R. J. Eden, University of California at Riverside report UCR-34P107-105 (1969).
6. A. Citron et al., Phys. Rev. 144, 1101 (1966). (This data was later revised. See G. Giacomelli et al., Hera Group Compilation, CERN report CERN/HERA 69-1.)
7. K. J. Foley et al., Phys. Rev. Letters 19, 330 (1967).
8. K. J. Foley et al., Phys. Rev. 181, 1775 (1969).
9. I. Mannelli et al., Phys. Rev. Letters 14, 408 (1965).
10. K. J. Foley et al., Phys. Rev. Letters 11, 503 (1963); C. Y. Chien et al., Physics Letters 28B, 615 (1969). We use the fit of the Particle Data Group, L. R. Price et al., UCRL 20000 K<sup>+</sup>N (September 1969).
11. K. J. Foley et al., Phys. Rev. Letters 15, 45 (1965); M. Aderholz et al., Physics Letters 24B, 434 (1967).

FIGURE CAPTIONS

- Fig. 1:  $\alpha$ , the ratio of real and imaginary parts of the various amplitudes discussed in the mathematical example of Section II. The subtraction constant  $c$  is chosen so that for  $\nu < \Lambda$ ,  $\alpha_I \approx \alpha_{II}$ .
- Fig. 2:  $\pi^\pm p$  total cross sections and fit (10). Errors plotted are the sum of the statistical and the systematic. The statistical errors of Allaby et al. are also indicated. The errors of Citron et al. are mainly systematic, and only representative data points of this group have been included.
- Fig. 3: Predicted  $\alpha(\pi^\pm p) = \text{Re } A(\pi^\pm p) / \text{Im } A(\pi^\pm p)$  and experimental data of Foley et al.<sup>8)</sup> I and II refer to the choice of high-energy cross sections. (See Fig. 2.)  $c$  is the subtraction constant.
- Fig. 4: Forward differential  $\pi N$  charge exchange cross sections predicted assuming exact I spin conservation, and data of Mannelli et al.<sup>9)</sup>
- Fig. 5: Blow-up of Fig. 4. The discrepancy between the fit and the data is an indication of the amount of I-spin violating electromagnetic effect. On the basis of this deviation, we conclude
- $$2\sigma_{EM}^{(-)} \lesssim 0.5 \text{ mb.}$$
- Fig. 6:  $\alpha(K^\pm p) = \text{Re } A(K^\pm p) / \text{Im } A(K^\pm p)$  and experimental limits deduced from the forward elastic differential cross sections.<sup>10,11)</sup> The sign of  $\alpha(K^\pm p)$  was determined from the dispersion relations. (See text.)

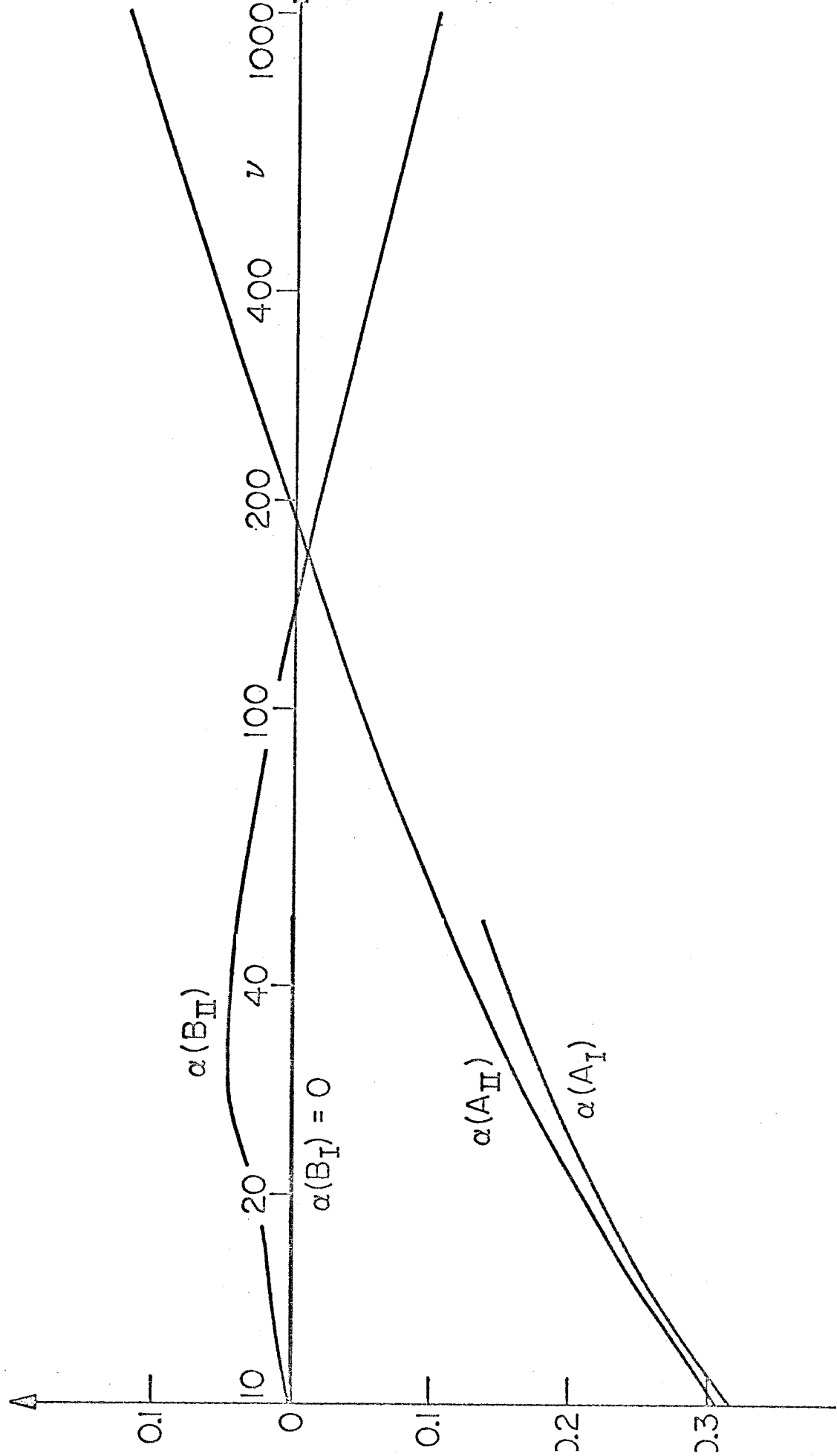


FIG. 1

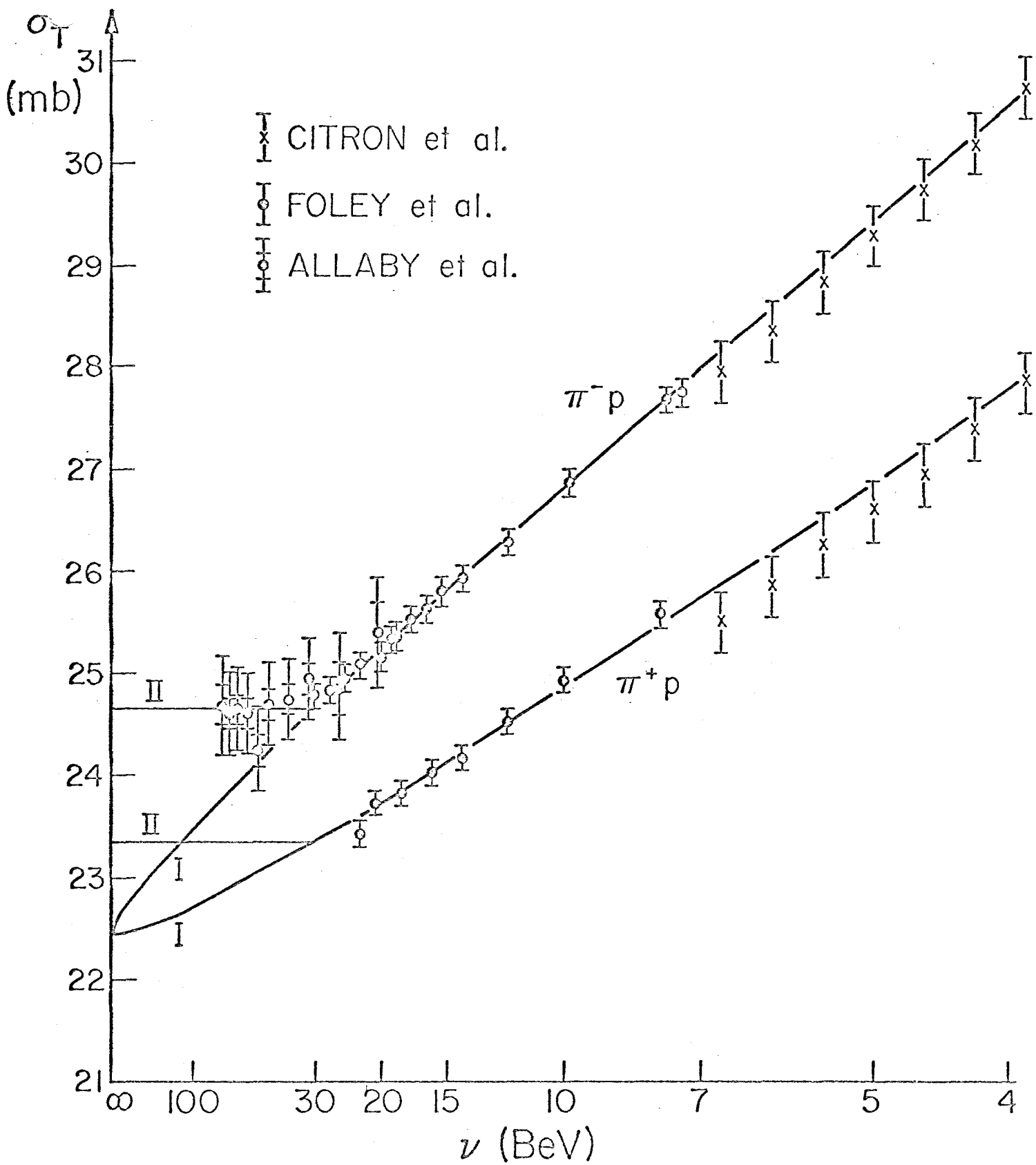


figure 2

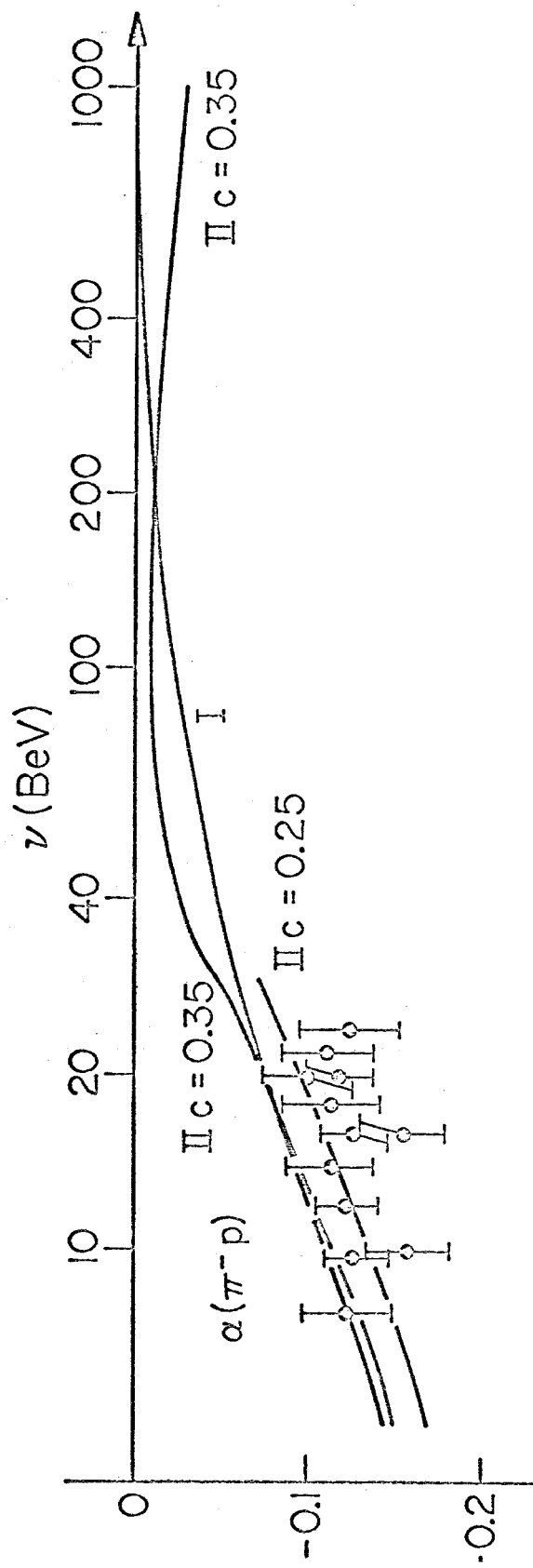
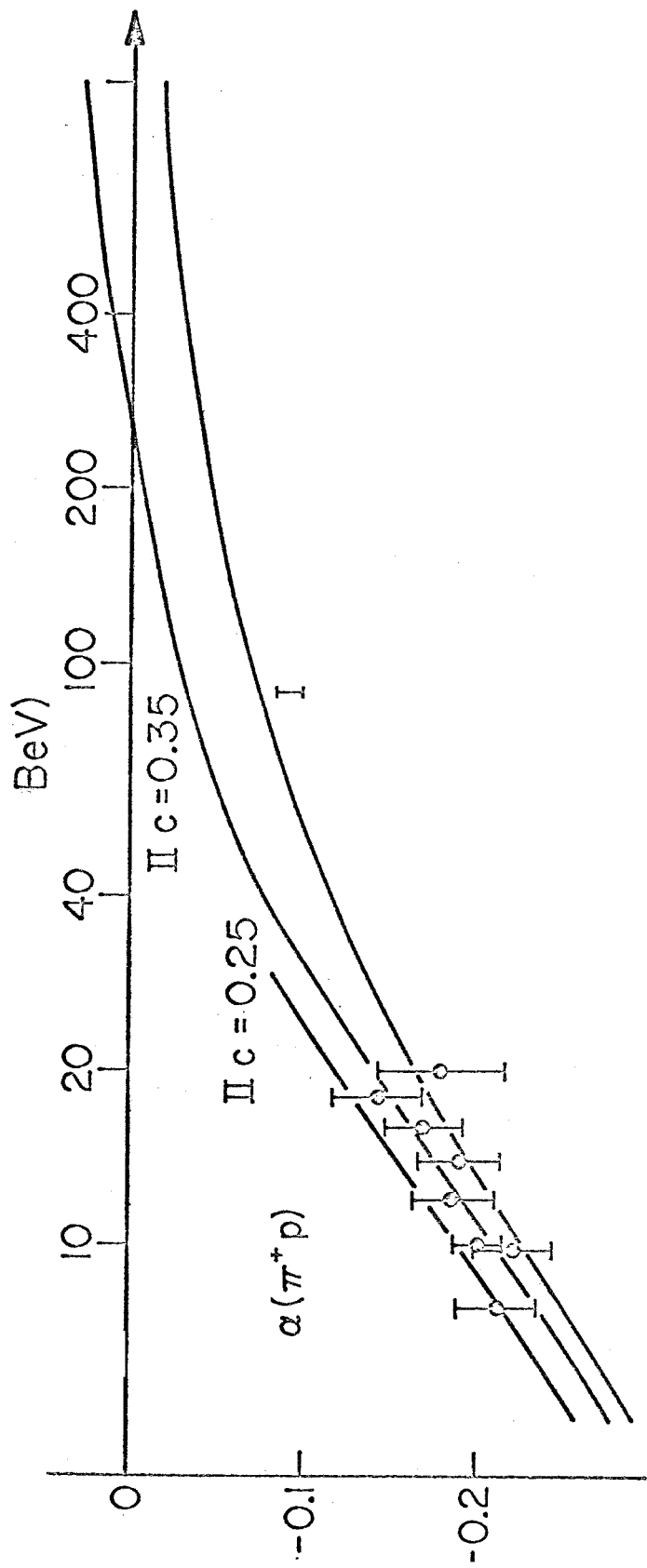


FIG. 3

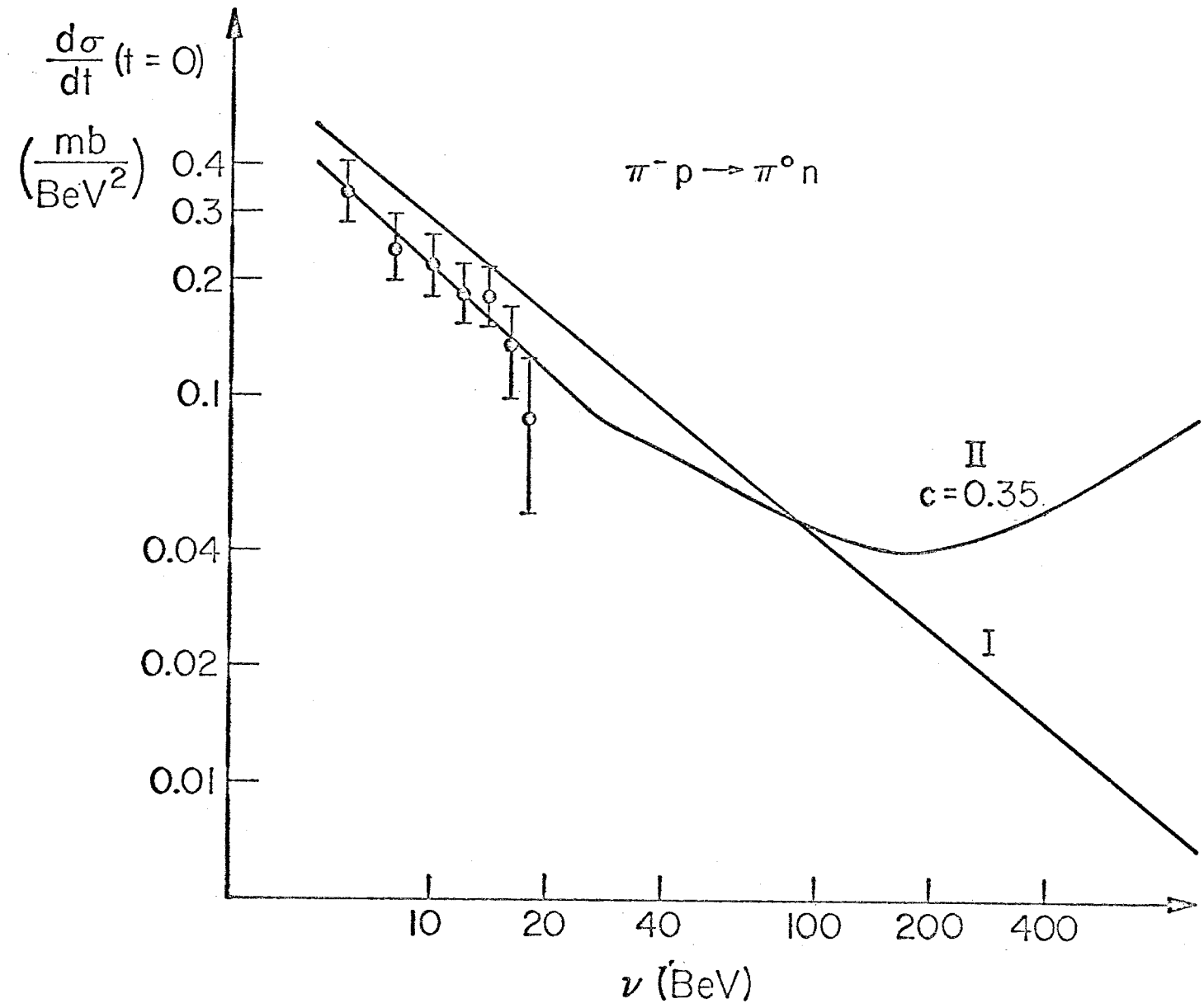


FIG. 4

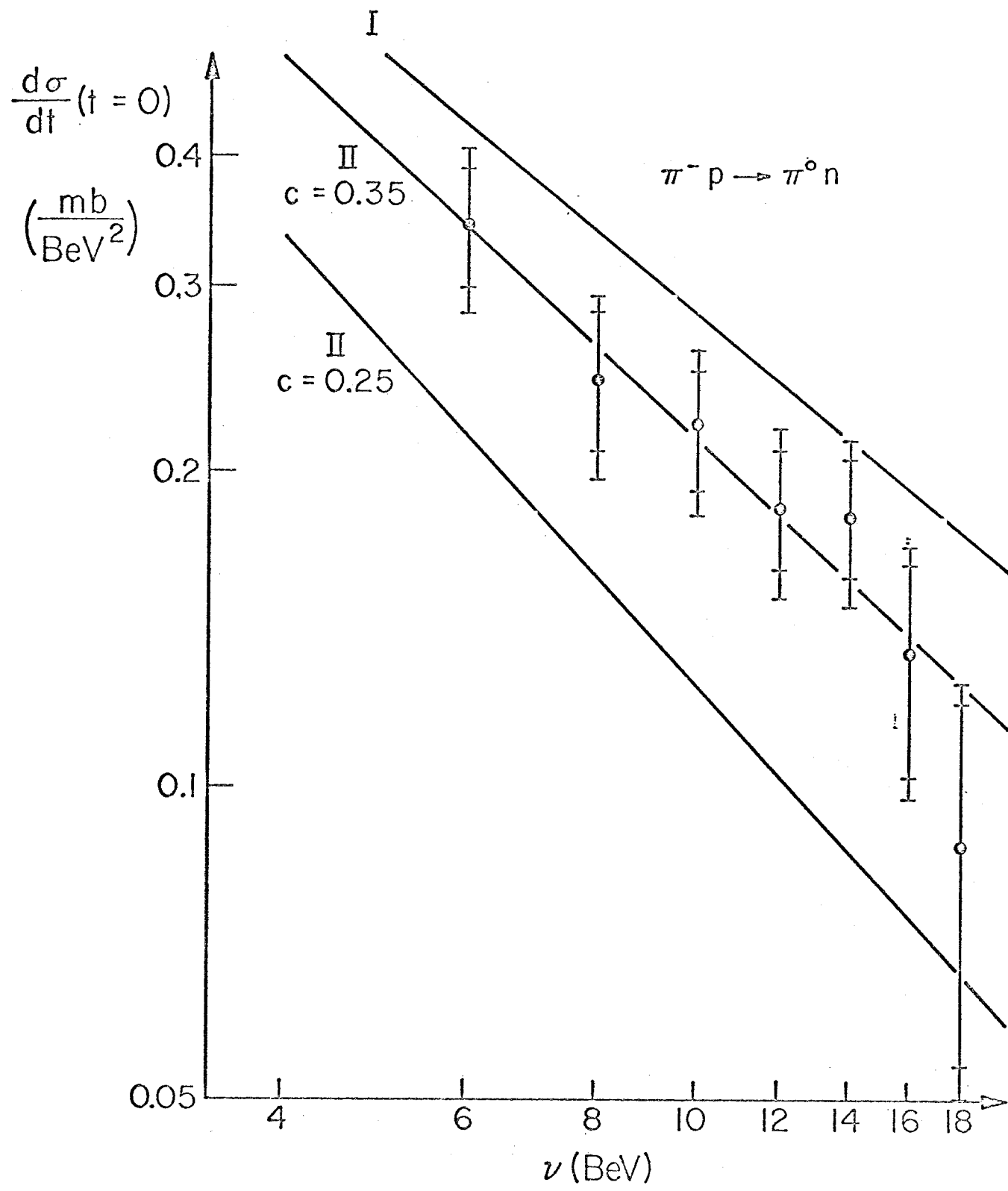


FIG. 5

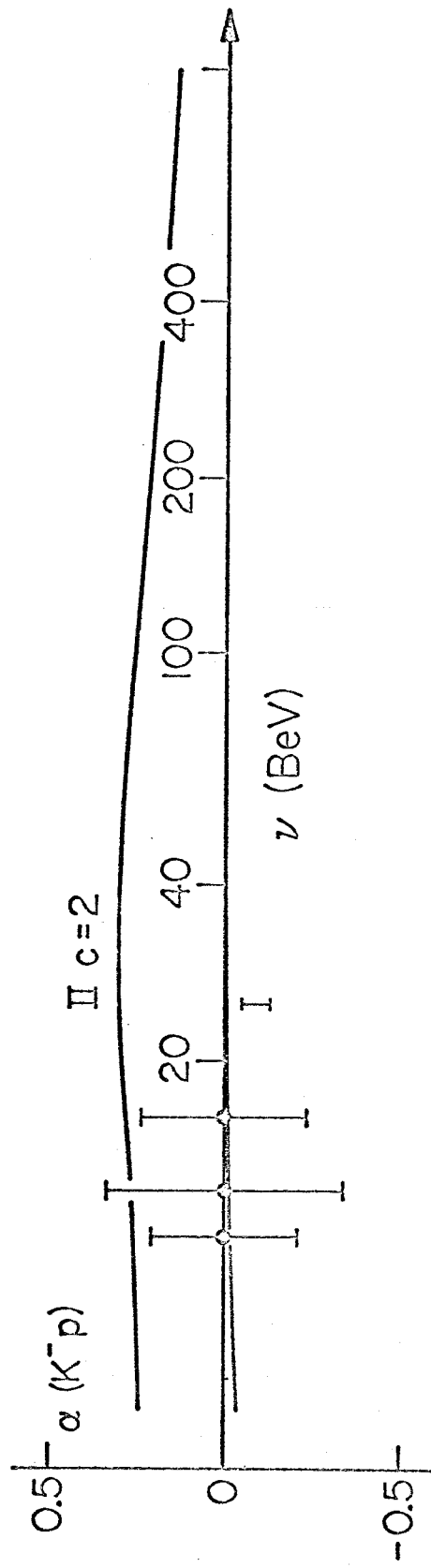
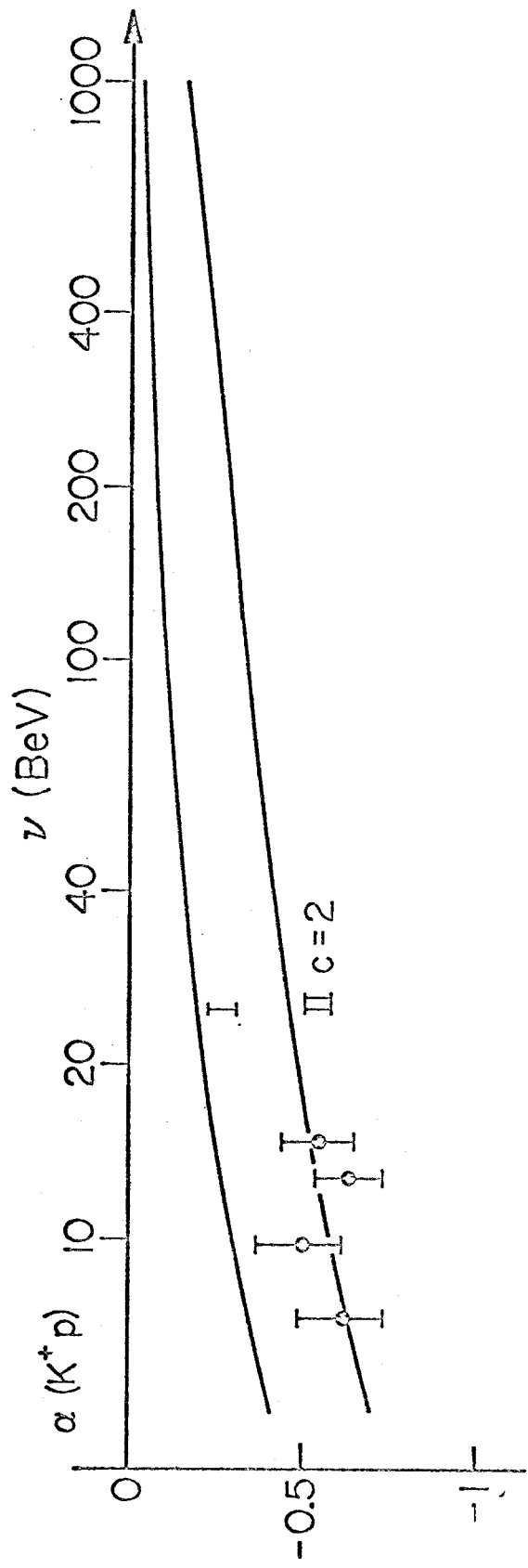


FIG. 6